УДК 621.0:621.3

MODELLING AND MAGNETIC FIELD SIMUALTION OF A TACTILE SENSOR BASED ON MAGNETO-SENSITIVE ELASTOMERS

[1]Simon Gast, [1]Klaus Zimmermann, [2]Vladimir T. Minchenya, [2]Victor G. Lysenko

[1]Technische Universität Ilmenau, Germany
[2]Belorussian National Technical University, Minsk, Belarus

Introduction. Common magneto-sensitive elastomers (MSE) consist of a silicon rubber matrix and ferromagnetic particles. The properties of this smart material are depending on the magnetic field, temperature and mechanical stress and can be influenced by other additives like silicon oil or graphite [1, 2]. Especially the magnetorheological effect (MR-effect), which describes the dependence of mechanical properties on the magnetic field, makes MSE suitable for applications as sensor or actuator [3, 4]. Furthermore, effects and properties like the field-dependent elongation (often called “magnetostriction”) or magneto resistivity of MSE are investigated [5, 10, 11]. Among others, the material is implemented into force-, magnetic field and acceleration sensors [6 - 9].

Kawasetsu et al. [12, 13] developed a tactile sensor using a planar coil and measuring the change of the inductance caused by a deformed and thereby approaching MSE layer. Thus, they measured the force and could differ between shear and compression with the help of multiple coils. They also investigated the planar sensitivity of one coil. In fact, the signal to noise ratio decreases with distance from the center region.

Since the field dependent properties can be tuned with a magneto-static field and the inductance measurement is performed with high frequency tank circuits, both methods may be combined. Considering this, a tactile sensor can be advanced with an adaptive part changing its elasticity.

The goal of this paper is, to present a first approach combining the measurement of change in magnetic permeability and controlling the field-dependent elasticity of the MSE (magneto-rheological-effect, MR-effect). Considering continuous recording of a deformation and a known field-elasticity-correlation, the elasticity of a penetrating object could be determined and recorded. In order to achieve a detailed understanding of this mechanism, the actuator and sensor function is firstly separated into two different layered components. In addition to this, a simple setup and mechanical model is used to create an initial approach for future derivatives and investigations. Taking elasticity estimation and the position dependency of sensitivity into account, an MSE based tactile sensor can be capable of detecting contact force, localizing and estimating the extent of the contact area as well as estimating elasticity of the penetrating object. In future research this sensor principal can be improved as artificial skin with extensive use.

Structure and function of the tactile sensor. In Figure 1, the elements of the tactile sensor are shown. In this setup, both the field stiffening (actuated layer) and the measuring part (sensing layer) are split into two separated components. A rigid spacer connects these parts. Thus, both layers are not affecting each other in an electromagnetic way. Firstly, this setup and the following simulations consider only isotropic MSE samples.

The sensing layer on top of the setup consists of a flexible planar coil as part of a tank circuit driven by its resonance frequency. It is known that changes in magnetic permeability near the flexible planar coil lead to a varying inductance. The LDC1614 EVM (Texas Instrumtens IC Evaluation Module) is measuring the change in resonance frequency of the

electrodynamic system. Since, the capacitance is maintained, the resonance frequency depends on the inductance and the measured frequency corresponds to the deformation.

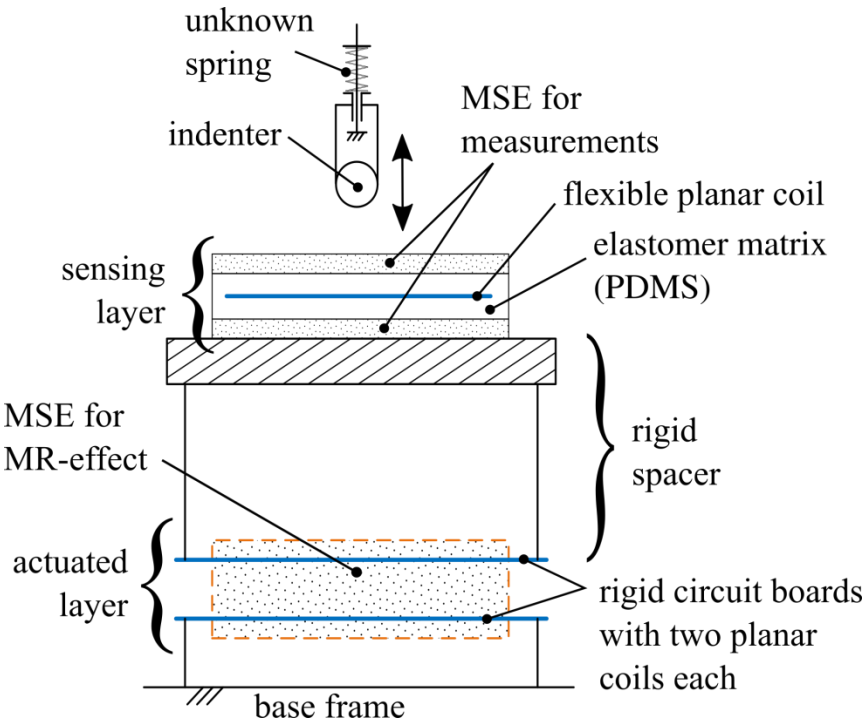

Fig. 1. Structure of the tactile sensor

Hence, the penetrating indenter results in an increase of inductance by pushing the MSE closer to the flexible coil. In contrast to the investigations of Kawasetsu et al. [12], an into the silicon matrix integrated flexible coil is used. On one hand, in this way the signal to noise ratio can be enhanced, since both sides experience an approaching of MSE. On the other hand, this leads to a bending of the coil itself, which lowers the inductance [18].

Various types of coils or magnet structures can produce a homogeneous field within the MR-effect actuated part. To obtain a variable flux density with a construction as small as possible, integrated planar coils are used. Therefore, the sensor setup consists of two rigid circuit boards with two parallel spiral coils, respectively, milled out of copper layers. Cast into PDMS and MSE it acts like an adjustable elasticity. In Fact, this arrangement is very similar to a Helmholtz coil couple.

The penetrating indenter at the top of the setup deforms both layers and is coupled elastically with the base frame. Firstly, this setups purpose is to determine the stiffness of a soft unknown spring at the indenter. Experimental investigations can deliver the relation between applied current and elasticity in the actuated layer. Knowing this elasticity-current-correlation and the present deformation in the sensing layer, a mechanical model is needed to estimate the stiffness of the spring. Considering the preferred low energy state of the particles, there should be a sinking current slope leading to a softening of the actuated layer. Since, MSE shows a memory shape effect when it is exposed to a magnetic field, an increasing current would not lead to an elongation of the MSE after deformation [16]. Consequently, a rising current slope would lead to a lower effective stiffening. Moreover, high currents may not cause great heating, when the current peak occurs after contact and is sinking fast in further progress.

Mechanical modelling of the sensor. The structure of the sensor is modelled as series of three springs (see Figure 2). For this simplification, it is assumed that there are only small deformations by the indenter. The elasticity of the two layers are henceforth considered as

springs. The magnetic field of the actuated layer controls the stiffness of the spring with spring rate c_D at the bottom through the MR-effect. The sensor spring (constant spring rate c_S) in the middle measures changes in length caused by the penetrating indenter in the sensing layer. For this model, only a central, uniaxial and collinear load on the spring system is assumed.

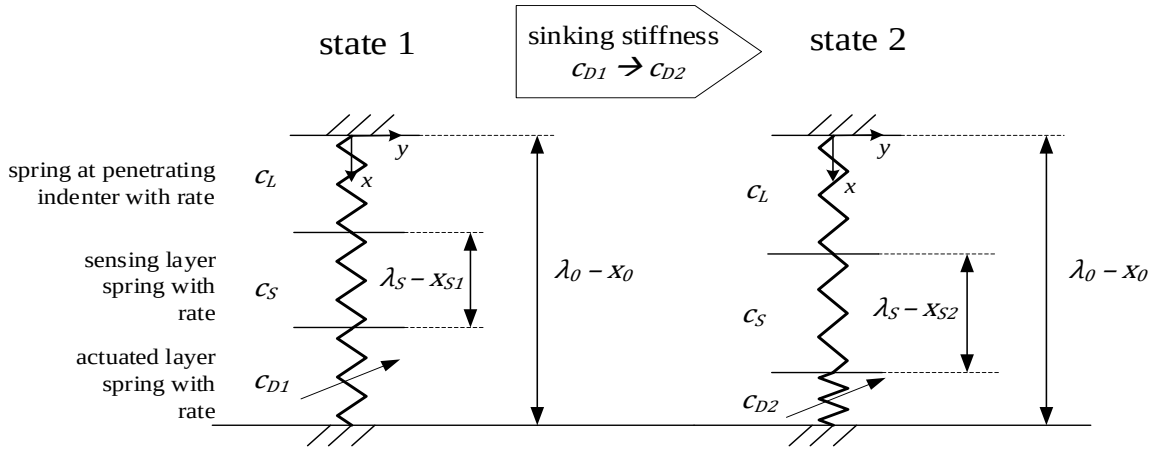

Fig. 2. Mechanical model as spring system

In Figure 2, λ_0 is the sum of all three relaxed spring lengths, λ_S is the relaxed spring length of the sensing layer spring, x_0 initial constant displacement of all springs and x_{S1} and x_{S2} the displacement of the sensor layer spring at different states. Knowing the correlation of stiffness and current in the actuated layer, the stiffness of the unknown spring (c_L) can be estimated. For this model, only quasi-static states and constant overall length $\lambda_0 - x_0$ are assumed. Hence, within the interval of changed spring length $x_{S1} - x_{S2}$, c_L can be determined by the following equations.

$$\frac{1}{c_1} = \frac{1}{c_L} + \frac{1}{c_S} + \frac{1}{c_{D1}} \qquad \frac{1}{c_2} = \frac{1}{c_L} + \frac{1}{c_S} + \frac{1}{c_{D2}} \tag{1}$$

$$c_L(x_{S2}) = \frac{c_S c_{D1} c_{D2} \cdot (x_{S1} - x_{S2})}{x_{S2}(c_{D1}c_{D2} + c_S c_{D1}) - x_{S1}(c_{D1}c_{D2} + c_S c_{D2})} \tag{2}$$

Where c_1 and c_2 are the spring rates for the spring system at state one and two. The stiffness of the actuated layer is limited by the maximum current that can be applied which limits the interval $[x_{S1}, x_{S2}]$. The maximum current itself is restricted by the requirement to avoid mechanical influences by heat. However, because of the continuous recording of $x_{S1} - x_{S2}$ and the current, this sensor can detect even nonlinear spring rates. From (1) it is assumed that $c_L$is of similar magnitude as c_S and c_D. Knowing c_S and c_D for different states, (2) is only depending on the deviation $x_{S1} - x_{S2}$.

Magnetic field simulation (MFS) and optimization of the actuated layer. The restrictions by using planar coils integrated into the actuated layer result generally in low flux densities. Moreover, it is challenging to obtain a homogeneous field with this setup. However, magnetic inhomogeneities or gradients within the MSE cause unwanted additional loads superposing the mechanical one by the indenter and lowering the effective stiffening. Nevertheless, special geometry designs lead to higher flux densities in certain regions. Since the mechanical stress is only applied on the MSE between the circuit boards, the obtained simulations tend to a concentration of the flux within this section.

In this paper, the magnetic field is optimized within the actuated layer of the sensor by enhancing the flux density and obtaining a homogeneous distribution. For all investigations, the ANSYS framework and Maxwell 3D Software is used. Figure 3 and Table 1 define the setup. In the electromagnetic model all coils are simplified by using only seven turns of conductive copper. Thus, the current density and filling ratio of the simulated coil can be maintained in comparison to the spiral planar coil. In all simulations, it is assumed that the MSE has a constant relative magnetic permeability of $\mu_r = 3.7$. Bastola and Schubert et al. [14, 15] have shown that this value corresponds to a CIP volume fraction of about 30%.

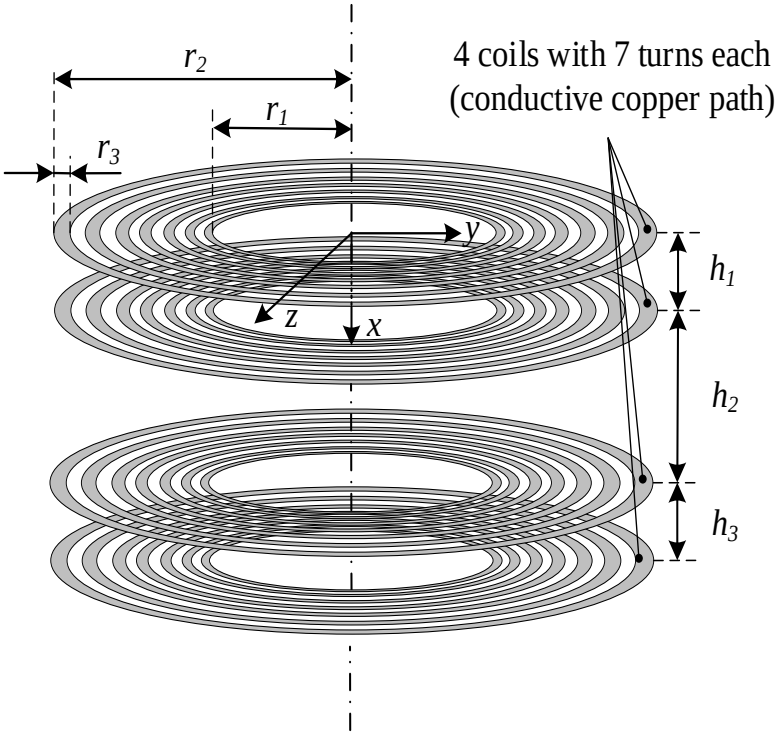

Fig. 3. Modell of the actuated layer for 3D MFS

The magnetic resistance for the volume with the cross section $y^2 + z^2 = R^2$, with $r_1 \leq R \leq r_2$ and the height 0.07mm $\leq x \leq$ 0.07mm + h_1 and 6.71mm $\leq x \leq$ 6.71mm + h_3 is simulated as diamagnetic material (circuit boards). The flux density is always plotted in the x-y-plane since the geometry is axially symmetric. The Figures 4, 5 and 6 show the flux density in case of completely in MSE cast circuit boards. The high flux densities maintain within the core and the adjacent regions. It can be expected that a geometry filling these regions only lead to higher flux densities, since the field is more concentrated. For this setup (completely cast into MSE) there are no sections of homogeneous flux distribution.

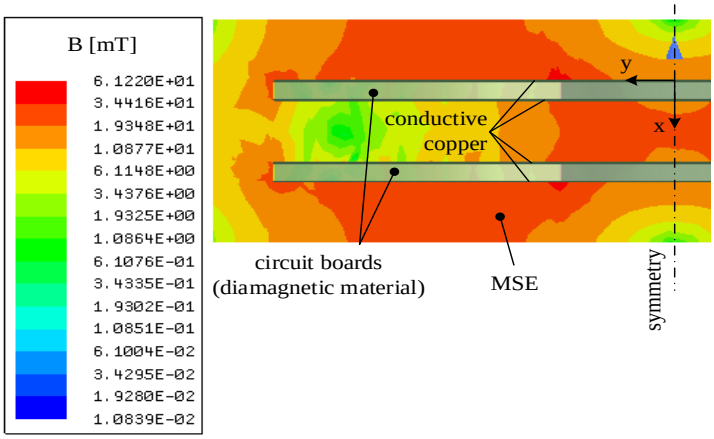

Table 1 – Parameters for MFS

Paramater	Value
r_1 [mm]	8
r_2 [mm]	28
r_3 [mm]	2
h_1 & h_3	1.5
[mm]	5
h_2 [mm]	70
Thickness	10
Cu [µm]	3.7
Current [A]	
μ_r	

Fig. 4. MFS of the actuated layer completely cast into MSE

As a first step, a geometry variation and its effect on field distribution and flux density for the layer setup is investigated. Figure 8 shows the proposed design that concentrates on the regions with high flux densities. This shape of the sample possesses curved surface parts to gain similarity to an ellipsoid-shaped body. Consequently, a more homogenous field is obtained, due to the boundary conditions of the magnetic field at the edges of a magnetized body. This can be considered as a design rule for MSE specimens. Sharp corners and discontinuities of the surface geometry always lead to inhomogeneous field distributions within the sample [17]. The corresponding chart in Figure 7 proves to have a slightly higher flux density. It also shows a more continuous trend in x-direction.

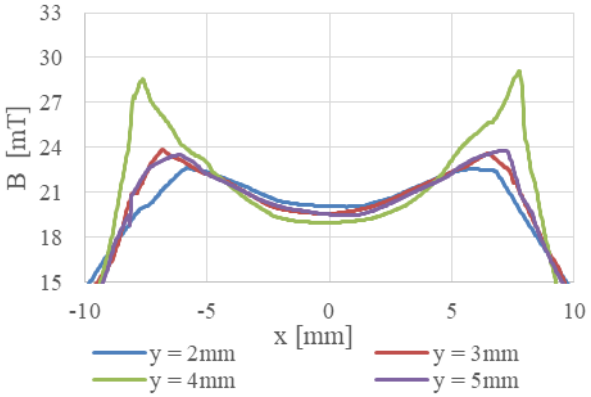

Fig. 5. Flux density plot parallel to y-axis, completely cast in MSE

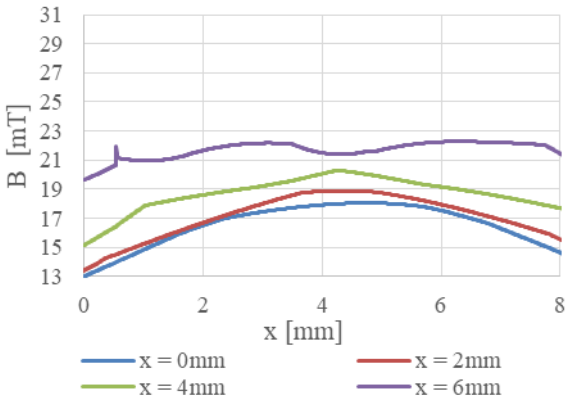

Fig. 6. Flux density plot parallel to x-axis, completely cast in MSE

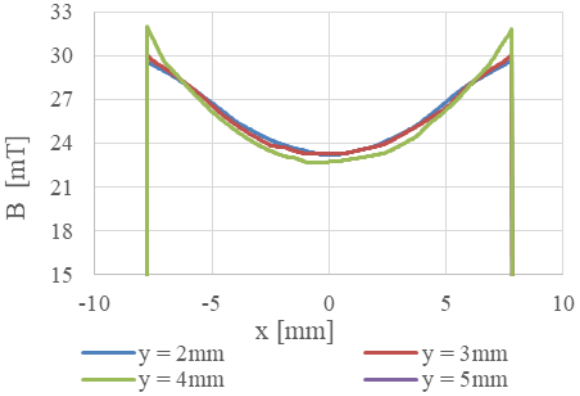

Fig. 7. Flux density plot parallel to y-axis for optimized geometry

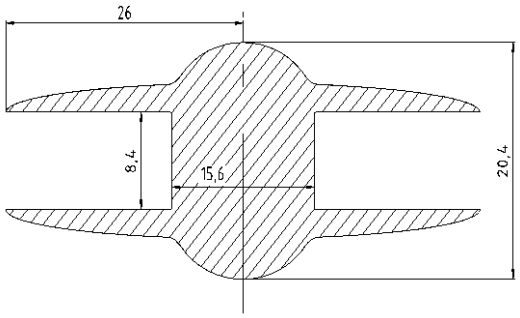

Fig. 8. Optimized geometry of the MSE

As a second step, high permeable plates covering the top and bottom cross section of the core are added to the MFS setup. Figure 11 shows the combination of the design variation and integration of permalloy plates (nickel-iron alloy, relative permeability up to 100 000) with a thickness of 0.3mm. These plates are considered to be cast into the MSE samples. In this way, a homogenization of the field and enhancement of the flux within the core section can be expected, since the magnetic flux is led through cross sections of least magnetic

resistance. As Figure 9 and 10 show, this bundling affects the flux significantly in such manner that a more homogeneous field is obtained.

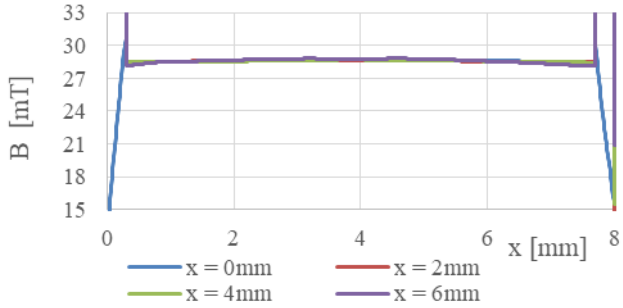

Fig. 9. Flux density plot parallel to x-axis with high permeable thin plates and optimized geometry

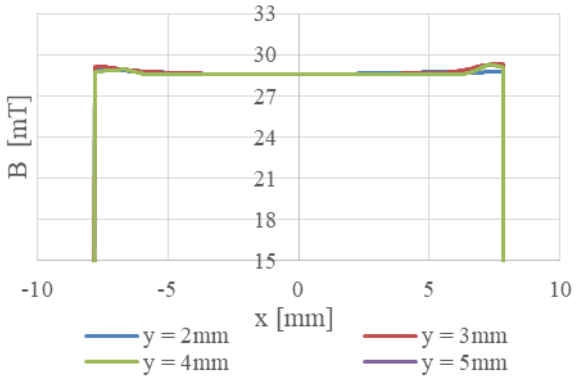

Fig. 10. Flux density plot parallel to y-axis with high permeable thin plates and optimized geometry

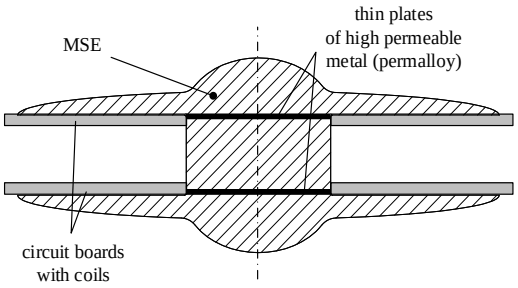

Fig. 11. Setup with high permeable thin plates

Conclusion and outlook. In this paper a concept of a tactile sensor setup is proposed to measure deformation and estimate stiffness of a penetrating object. With restrictions and an analogous spring model, the sensor equation is derived from only two indicators. Thus, it is shown that with a known stiffness-current-correlation and measured deformation, the stiffness of a soft unknown spring can be obtained. Subsequent the range of adjustable stiffness for the actuated layer is of particular interest. Therefore, two different optimization steps for obtaining an enhanced and homogenized flux within the core section of our proposed sensor setup are investigated. The MSE geometry of the simulation is varied and thin plates of permalloy are added. As a result, an improved field distribution within the core section of the actuated layer setup is obtained.

In future research, experimental investigations of this setup are intended. For instance, the unification of the actuated and sensing layer is of particular interest. Considdering the proposed sensor as an artificial skin, it is also important to develop a distributed stiffening instead of a regional concentrated one. In addition to that, the sensing layer with its planar sensitivity depending on the contact position offers potential for a localization of the contact within the sensor area. Furthermore, a comparison through experimental investigations may prove the assumption that a constant magnetic field will not affect the alternating one of the resonating circuit. Another investigations could be done, comparing an in MSE enclosed coil with an undeformed one.

REFERENCES

1. *K. Zimmermann, V. Boehm, T. Becker, G. Monkman et al., T "Mechanical Characterization of the Field-Dependent Properties of Magnetoactive Polymers and Integrated Electrets for their Application in Soft Robotics", Problems of mechanics, vol. 4, pp. 5-17, 2017*
2. *V. A. Naletova, D. A. Pelevina, et al., "Bi-stability of the deformation of a body with a magnetizable elastomer in a magnetic field", Magnetohydrodynamics, vol. 52, pp. 357-368, 2016*
3. *L. Bodelot, J.-P Voropaieff, T. Pössinger, "Experimental investigation of the coupled magneto-mechanical response in magnetorheological elastomers", Experimental Mechanics, vol. 58, pp. 207–22, 2018*
4. *T.I. Becker, K. Zimmermann, D.Yu. Borin, G.V. Stepanov, P.A. Storozhenko, "Dynamic response of a sensor element made of magnetic hybrid elastomer with controllable properties", Journal of Magnetism and Magnetic Materials, vol. 449, pp. 77-82, 2018*
5. *Yancheng Li, Jianchun Li, Weihua Li and Haiping Du, "A state-of-the-art review on magnetorheological elastomer devices", smart materials and structures, vol. 23, p. 123001, 2014*
6. *B. Yoo, S. Na, A. B. Flatau and D. J. Pines, "Evaluation of Magnetorheological Elastomers With Oriented Fe–Ga Alloy Flakes for Force Sensing Applications", in IEEE Transactions on Magnetics, vol. 52, no. 7, pp. 1-4, 2016*
7. *W. Li, K. Kostidis, Xianzhou Zhang and Yang Zhou, "Development of a force sensor working with MR elastomers," 2009 IEEE/ASME International Conference on Advanced Intelligent Mechatronics, Singapore, pp. 233-238, 2009*
8. *S. Qi, H. Guo, & J. Chen, et al., "Magnetorheological elastomers enabled high sensitive self-powered tribo-sensor for magnetic field detecting". Nanoscale, vol. 10, pp. 4745–4752, 2018*
9. *I. Tomčíková, M. Bereš, I. Kováčová and V. Melnykov, "Interaction between magnetic and stress field in ferromagnetic core of magnetoelastic pressure force sensor", 2017 International Conference on Modern Electrical and Energy Systems (MEES), Kremenchuk, pp. 124-127, 2017*
10. *W. H. Li, T. F. Tian and H. Du, "Sensing and Rheological Capabilities of MR Elastomers", Smart Actuation Sens. Syst. - Recent Adv. Futur. Challenges, pp. 249–279, 2012.*
11. *Y. Han, A. Mohla, X. Huang, et al., "Magnetostriction and field stiffening of magneto-active elastomers" Int. Journal of Appl. Mech., Vol. 7, p. 155, 2015*
12. *T. Kawasetsu, T. Horii, H. Ishihara and M. Asada, "Size dependency in sensor response of a flexible tactile sensor based on inductance measurement", in IEEE Sensors Journal 2017, Glasgow, pp. 1-3, 2017*
13. *T. Kawasetsu, T. Horii, H. Ishihara and M. Asada, "Flexible Tri-Axis Tactile Sensor Using Spiral Inductor and Magnetorheological Elastomer", in IEEE Sensors Journal, vol. 18, no. 14, pp. 5834-5841, 2018*
14. *G. Schubert, P. Harrison, "Magnetic induction measurements and identification of the permeability of Magneto-Rheological Elastomers using finite element simulations", Journal of Magnetism and Magnetic Materials, vol. 404, pp. 205-214, 2016*
15. *A.K. Bastola, M. Paudel, L. Li, "Magnetic circuit analysis to obtain the magnetic permeability of magnetorheological elastomers", Journal of Intelligent Material Systems and Structures, vol. 29, pp. 2946-2953, 2018*
16. *J. Chavez Vega, T. Kaufhold, V. Böhm, T. Becker, K. Zimmermann, et al., "Field-induced plasticity of magneto-sensitive elastomers in context with soft robotic gripper applications", Proc. Appl. Math. Mech., vol. 17, pp. 23-26, 2017*

17. *J. A. Osborn "Demagnitizing Factors of the General Ellipsoid", Phys. Rev., vol. 67, pp. 351-357, 1945*
18. *G. Fotheringham, F. Ohnimus et. al., "Parameterization of Bent Coils on Curved Flexible Surface Substrates for RFID Applications", 59th Electronic Components and Technology Conference, San Diego, CA, pp. 502-507, 2009*